Growing forced bars determine non-ideal estuary planform

J.R.F.W. Leuven[1], L. Braat[1], W.M. van Dijk[1], T. de Haas[1] and M. G. Kleinhans[1]

[1] Faculty of Geosciences, Utrecht University, PO-box 80115, 3508 TC Utrecht, The Netherlands

Key Points:

- Forced mid-channel bars cause bank erosion leading to a quasi-periodic estuary planform
- Self-formed confinements separate zones in which the estuary is wider and bars are more dynamic
- Confinement spacing scales with bar dimensions and estuary width in experiments and nature

Corresponding author: Jasper R.F.W. Leuven, `j.r.f.w.leuven@uu.nl`

Abstract

The planform of estuaries is often described with an ideal shape, which is exponentially converging in landward direction. We show how growing forced bars determine the large-scale estuary planform, which explains the deviations from the ideal planform for natural estuaries filled with bars. Experiments were conducted in a 20 m long, 3 m wide tilting flume, the Metronome. From a narrow, converging channel a self-formed estuary developed characterised by multiple channels, braided bars, a meandering ebb channel and an ebb delta. Bars hardly migrated due to the alternating current, but the bar width increased with increasing estuary width. At locations where the estuary width was narrow, major channel confluences were present, while the zones between the confluences were characterised by a higher braiding index, periodically migrating channels and a relatively large estuary width. At the seaward boundary, confluences were forced by the presence of the ebb-tidal delta. Diversion of flow around forced mid-channel bars causes bank erosion and the estuary self-confines at other locations by sidebar formation. This results in a planform shape with a quasi-periodic widening and narrowing at the scale of forced bars. Observations in natural systems show that major confluence locations can also be forced by inherited geology and human engineering, but otherwise the estuary outline is similarly affected by tidal bars. These observations provide a framework for understanding the evolution of tidal bar patterns and its planform, which has strong implications for navigation, dredging and ecology.

Keywords: estuaries; bar pattern; channel configuration; channel dynamics; scale-experiment; long-term evolution

1 Introduction

Estuaries are tidal systems that occur where rivers debouch into the sea. The planform of estuaries is often described by an ideal shape [*Pillsbury*, 1956; *Langbein*, 1963; *Savenije*, 2015], which is defined as an equilibrium state wherein the channel planform is converging with a constant along-channel tidal range, average depth and current velocity amplitude. While this concept applies well to delta branches and tidal creeks, previous research showed that the planforms of alluvial estuaries are rather irregular than ideal [*Leuven et al.*, 2017] (Figure 1). Deviations from the ideal shape may occur because the estuary adapted in varying degrees to its equilibrium shape, depending on the time and sediment available to adapt to changing boundary conditions, such as Holocene sea-level rise and antecedent topography [*Townend*, 2012; *de Haas et al.*, 2017]. In addition, the outline may be shaped by external restrictions that impose local confinements, such as inherited geology or human engineering, as well as self-formed restrictions, such as salt marshes and riparian forest [*Townend*, 2012] (Figure 1). Current theoretical and empirical descriptions for estuary planform neglect the effect that bar formation and bar evolution may have on the planform of the estuary. We propose that the irregular planform of many alluvial estuaries is shaped by a forcing mechanism in which growing mid-channel bars determine boundary erosion, leading to quasi-periodic widening and narrowing of the estuary.

In contrast to tidal systems, the forcing mechanism of bars has been thoroughly studied for river systems. For rivers, it was found that small alternate bars may cause channel curvature, after which the alternate bars evolve into point bars, forcing a meandering planform [*Schuurman et al.*, 2016]. The location and size of forced bars may be caused by channel width and discharge variation, for example due to the presence of embayments [*Struiksma et al.*, 1985; *Tubino et al.*, 1999; *Repetto and Tubino*, 2001; *Seminara*, 2010; *Wu et al.*, 2011; *Kleinhans and van den Berg*, 2011; *Schuurman et al.*, 2013]. This suggests an intimate link between bars and river planform, and we hypothesise a similar dependency between tidal bars and estuary planform. Indeed, observations in natural estuaries support the hypothesis that the location where tidal bars occur can be predicted by the deviation of the estuary planform from an ideal shape [*Leuven et al.*, 2017, 2018]. In addition, bar dimensions scale with estuary width (bar length $\propto$ channel width$^{0.87}$, *Leuven et al.* [2016]). From aerial photographs one can observe that

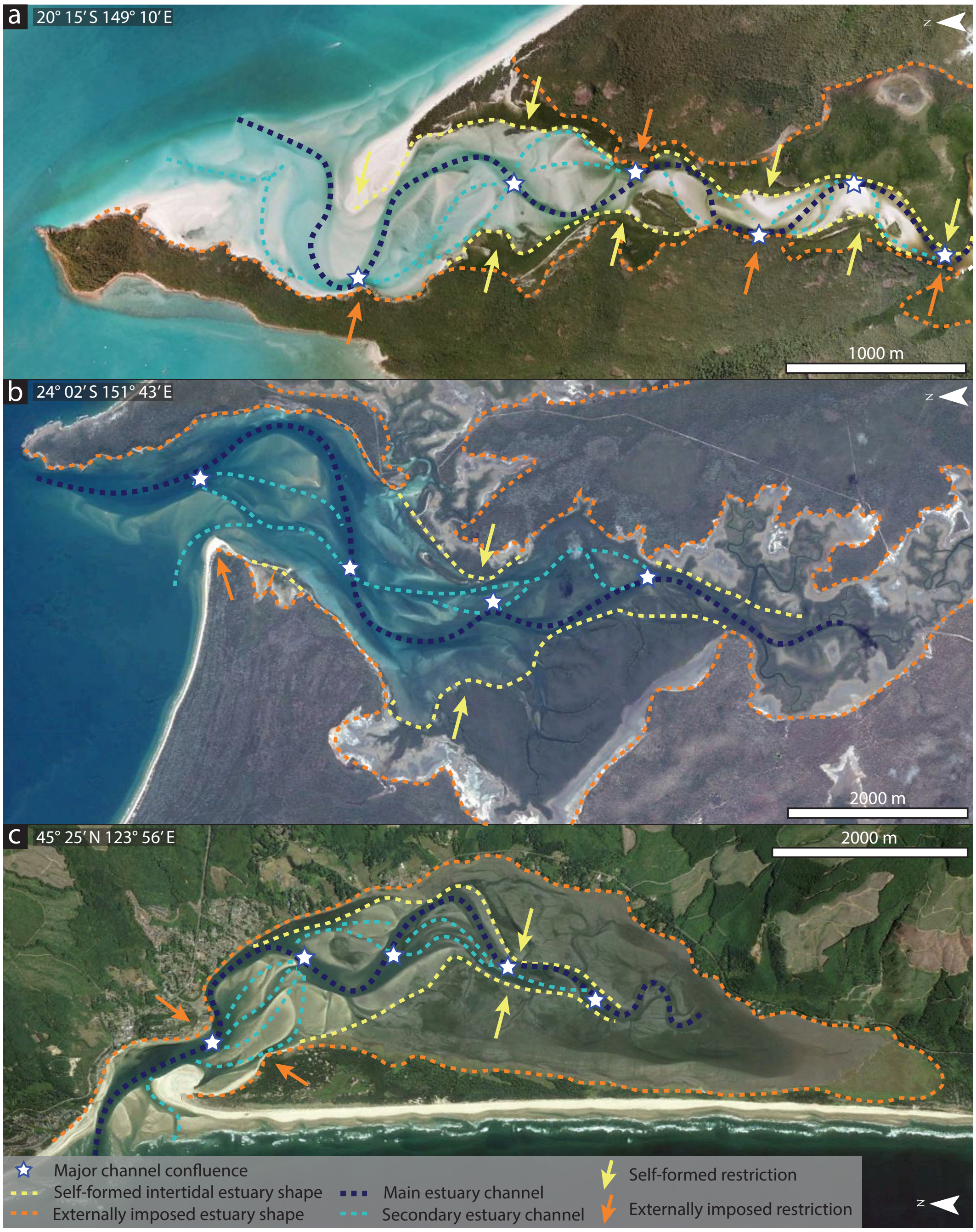

Figure 1. Aerial photographs of (a) Whitehaven beach (Aus), (b) Rodds Bay (Aus), and (c) Netarts estuary (USA). The outline of these estuaries shows an irregular rather than ideal converging shape. Local confinements occur due to externally imposed restrictions, such as bedrock geology and human engineering, as well as by self-formed restrictions. The deepest channels and major confluences occur at locations of confinement. Google Earth, accessed January-April 2017.

the locations where the estuary is relatively narrow correspond to locations where major confluences and the deepest parts of the main meandering channel occur (Figure 1). For braided rivers, the dimensions and spacing of confluences scale with bar dimensions [*Ashmore*, 2001; *Hundey and Ashmore*, 2009]. Confluence locations associated to downstream bifurcations steer the morphodynamics of channels and bars [*Schuurman and Kleinhans*, 2015]. For example, the deposition of a mid-channel bar downstream of a confluence location can create a bifurcation and subsequently erode the channel banks, creating a more irregular planform [*Hundey and Ashmore*, 2009; *Schuurman and Kleinhans*, 2015].

The forcing mechanism between bars and river planforms raises the question how the forcing of mid-channel bars in estuaries determines the large-scale widening and narrowing of the estuary outline. Current knowledge on long-term evolution – time-scales larger than decades – of bars and channels in estuaries is limited by a lack of data [*de Haas et al.*, 2017]. Numerical models can produce realistic long-term evolution of estuaries [*van der Wegen and Roelvink*, 2012; *Braat et al.*, 2017], but the produced channel and bar patterns are largely dependent on calibration parameters such as the transverse bed slope effect [*Baar et al.*, 2018]. Therefore, in this study we will use physical experiments instead.

For physical experiments of estuaries, we use a periodically tilting flume that generates dynamic tidal morphology. It produces hydrodynamic conditions capable of transporting sediment during both the ebb and flood phase [*Kleinhans et al.*, 2015a, 2017a], which is unique compared to former physical experiments of tidal systems that relied on periodic sea-level variations [*Reynolds*, 1887, 1889; *Mayor-Mora*, 1977; *Tambroni et al.*, 2005; *Stefanon et al.*, 2010; *Vlaswinkel and Cantelli*, 2011]. These experiments were hampered by the flood flow being too weak to transport sediment in landward direction and thus resulted in net exporting systems [*Kleinhans et al.*, 2014a]. Scaled estuary experiments thus require a much steeper bed gradient than natural systems, because of their smaller water depth and bed shear stress [*Kleinhans et al.*, 2014a, 2015a]. The tilting flume allows us to test our hypotheses regarding the long-term dynamics of channels and bars and to characterize the spatio-temporal patterns of channel and bar evolution.

Here, we explore the relation between channel and bars dynamics and estuary planform. In particular, we assess whether channel and bar dynamics can cause the often observed irregular estuary planform and the locations of major channel confluences. We test two alternative hypotheses for these observations: (i) the confluences are forced by the outline, which means that the outline sets the channel and bar pattern or (ii) the typical bar length forces the location of confluences, which implies that the bar pattern forces the outline of the estuary. In case the later hypothesis is valid, it is expected that a quasi-periodic estuary planform will evolve in self-formed estuaries. The results from this study provide a framework for future studies on the occurrence of mutually evasive ebb- and flood tidal channels as well as for natural channel and bar dynamics.

This paper is organized as follows: firstly, the methodology for the physical scale-experiments is given as well as the data collection from natural systems. Secondly, we present the evolution of a self-formed estuary in the experiments. Finally, the results from the experiment are compared with data collected from natural systems and a conceptual framework is presented that describes channel and bar patterns in estuaries.

2 Methods and materials

2.1 Experimental set-up and procedure

The experiments were conducted in a periodic tilting flume of 20 m by 3 m, called the Metronome, which enables transport of sediment during both the ebb and flood phase by tilting over the short central axis [*Kleinhans et al.*, 2017a] (Figure 2). Tidal currents were produced by four actuators that ensured a repeatable tilting with a period of 40 s and a maximum tilting gradient of 0.008 m·m^{-1}. For a more detailed description of the design and hydrodynamics of the Metronome see *Kleinhans et al.* [2017a].

Here, we describe one of the experiments with detailed monitoring of the bed elevation and flow velocities and study the long-term evolution of channels and bars. The experiment was run for 15000 tidal cycles, which corresponds to approximately 20 years of natural tidal cycles assuming a semi-diurnal tide. The experimental settings were selected based on a set of approximately 30 experiments in which initial and boundary conditions have been varied systematically. It was tested whether the settings were such that sediment was well above threshold for motion and that the tidal excursion length was shorter than the flume length.

A plane bed of 0.07 m thick sediment was installed on top of a mat with artificial grass in the basin. Sediment consisted of a sand mixture (ρ_s = 2650 kg·m^{-3}) with a median grain size of 0.52 mm and a coarse tail (D_{90}=1.2 mm, D_{10}=0.33 mm) (Supplementary Figure 1). This sediment mixture was selected to prevent the occurrence of scour holes as much as possible [*Kleinhans et al.*, 2014b, 2017b]. The bed was approximately 18 m long and 3.0 m wide. An initial channel was carved in the sediment bed to facilitate the initial flow from the upstream boundary to the sea and back. This initial channel was 0.03 m deep and the width increased exponentially from 0.2 m at the river to 1.0 m at the seaward boundary (Figure 2b).

At the upstream boundary water discharge was added to the flume during the ebb phase at a constant rate of 0.1 L· s^{-1}. River discharge was disabled during the flood phase, because otherwise water would pile up at the upstream boundary, resulting in an extreme water pulse when tilted seaward again. The water level at the boundary between the sea and the land was kept at a fixed elevation by a constant head at the downstream boundary of the flume, allowing free in- and outflow of water. Water depth in the sea was continuously compensated for the tilting of the flume, such that the water depth at the boundary between the sea and the estuary was always 0.065 m. Paddle-generated waves were introduced at the seaward boundary with a frequency of 2 Hz and an amplitude of approximately 3 mm during the flood phase. Waves were only introduced during the flood phase, because only in that phase the stirring of sand by the waves would cause sediment transport in landward direction. The water was dyed blue with Brilliant Blue FCF colourant to enhance the visualisation of morphology.

2.2 Data collection and data processing

Time-lapse imagery from seven overhead cameras was collected each tidal cycle at the horizontal position of the flume when transitioning from ebb to flood flow. The cameras were mounted at equal distances 3.7 m above the centreline of the flume. The CMOS MAKO colour cameras have a resolution of 2048 by 2048 pixels and a fixed focal length of 12.5 mm. The resulting spatial pixel resolution was 1.5-2 mm. Images were rectified and warped before they were stitched, and then converted to LAB (CIELAB) images, in which L represents the colour band with light intensity, A represents red to green and B yellow to blue [also used in *van Dijk et al.*, 2013]. The B-band was extracted from the LAB images, because it enhances the visualisation of morphology by the largest contrast between coloured water and sediment.

The flume was illuminated at about 600 lux with daylight-coloured fluorescent light aimed at a white diffusive ceiling at approximately 4.5 m above the flume floor. Light reflection from the water surface on the photographs was largely prevented by white photography backdrop cloth between the ceiling and flume to minimise reflection.

To create Digital Elevation Models (DEMs), photographs were taken with a digital single-lens reflex (DSLR) camera and processed with structure from motion software [*Lane et al.*, 1993; *Chandler et al.*, 2001; *Westoby et al.*, 2012; *Fonstad et al.*, 2013; *Morgan et al.*, 2017; *Agisoft and St Petersburg*, 2017]. The first 5 DEMs were made with an interval of 500 tidal cycles, starting at 300 cycles. Subsequently, 7 DEMs were made with an interval of 1000 cycles and the final 3 had an interval of 2000 cycles. The DEMs were referenced with 20 ground control points at

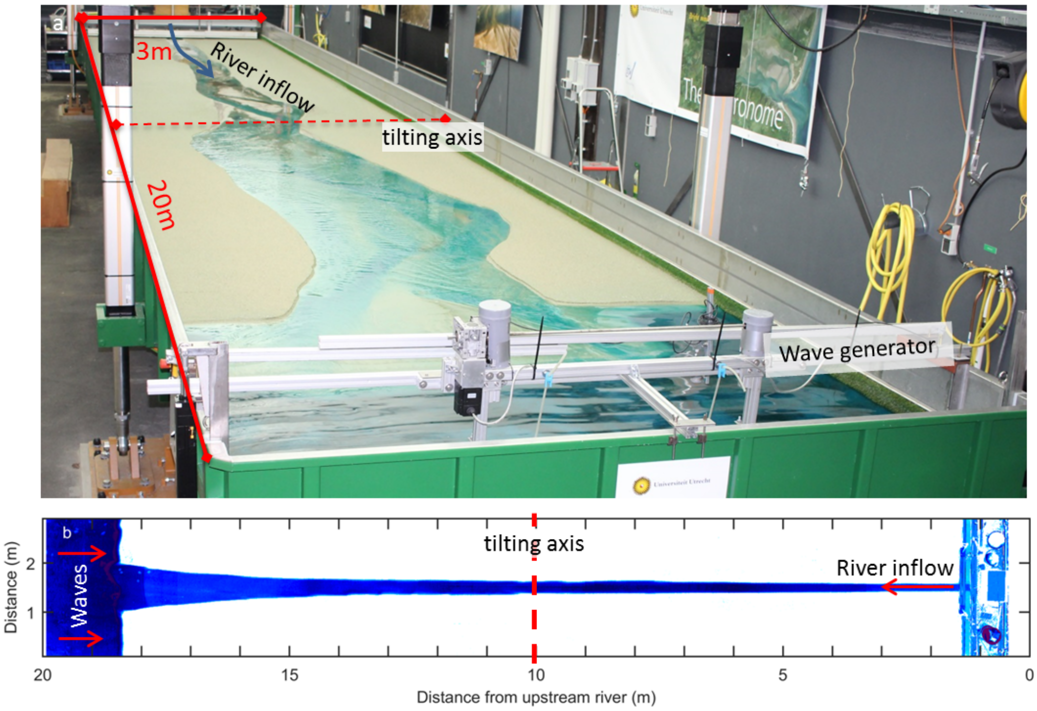

Figure 2. (a) The Metronome, a tilting flume of 20 m long by 3 m wide. (b) Overhead image of initial converging channel bathymetry. Blueness indicates depth except in the first meter where the gantry is located. Channel and bar patterns evolved over 15000 tilting cycles. At the landward side, river discharge ($0.1\ \mathrm{L \cdot s^{-1}}$) was added during the ebb phase. At the seaward end, paddle-generated waves were applied during the flood phase.

equal spacing on the sides of the flume, such that the resulting DEMs could be resampled on the same grid as the stitched images from the overhead cameras.

Flow velocities were measured over a tidal cycle with Particle Imaging Velocimetry (PIV) [*Mori and Chang*, 2003] at 12 moments during the experiment. These 12 moments correspond with the timing of the first 12 DEMs. White floating particles (diameter ca. 2.5 mm) were seeded on the water surface and resupplied when necessary. At 16 equally spaced phases of the tide, ten images were collected with the overhead cameras at 25 Hz, using a pulse train from a frequency generator. Flow velocities were subsequently calculated from pairs of consecutive images with the MPIV toolbox in Matlab [*Mori and Chang*, 2003]. As in *Kleinhans et al.* [2017a], we used the peak cross-correlation algorithm to determine mean particle displacement in pixels in a 50x50 window with 50% overlap. The resulting vector fields were scaled to metrics with the pixel footprint of the cameras (1.5-2 mm per pixel), correcting for the tilt of the flume. Erroneous vectors were obtained and filtered out where particles were sparse or overly-abundant, as well as when the PIV-window partly covered the flume wall or reflection on the water surface was too large. For processing, the average vector field was calculated for each tidal phase from ten consecutive images and for plotting purposes it was interpolated on a grid with the same size and resolution as used for the overhead cameras and DEMs. Residual currents were calculated as the average flow vector over a full tidal cycle.

2.3 Data reduction

Experimental results are compared with data from natural systems [*Leuven et al.*, 2016] to assess how well the tidal bars in our experiment scale to nature. A detailed comparison is made with the Western Scheldt (NL), for which detailed bathymetries over time and flow velocities are available. In this study, the important scaling properties are the planform dimensions of bars and the elevation distribution of the bathymetry. Therefore, maximum bar length and width were measured in the experiments following *Leuven et al.* [2016]. Hypsometric curves, which are cumulative depth elevation curves, were calculated for four zones in the experiment as well as for the Western Scheldt. These zones were chosen as the part between two successive width confinements in the estuary (Figure 3k, Supplementary Figure 6a).

Estuary width was measured in our experiment as the local width between the non-eroded estuary banks. Channel width was measured as the width of the estuary below an along-channel linear profile that was fitted on the median bed level per cross-section, whereas above the median bed level was classified as bar [see *Leuven et al.*, 2017, for method]. Excess width is defined as the estuary width minus the width from an ideal converging estuary shape [*Leuven et al.*, 2018] and summed width of bars was measured as the sum of the width of all bars in a cross-section [*Leuven et al.*, 2017].

The locations of major channel confluences and the spacing between them over time were determined for the experiment and the Western Scheldt. In addition, these quantities were measured on aerial imagery for a fixed moment in time in 7 other natural systems: Dovey (UK), Bannow (UK), TawTorridge (UK), Teign (UK), Rodds Bay (Australia), Whitehaven beach (Australia) and Netarts (USA). In case of aerial photographs, major confluence locations were visually determined as the deepest scour points where multiple channels converge, while these points were extracted from bathymetric data for the experiments and Western Scheldt (Figure 4). Deep scours as a result of bank protection or resistant layers that consist of shell fragments (so called 'crags', *Cleveringa* [2013]) were excluded for the Western Scheldt bathymetry. Subsequently, the location and spacing between successive channel confluences were measured with respect to local zones of confinement in the estuary outlines. Estuary outlines and along-channel width profiles as presented in *Leuven et al.* [2017] were used to determine the local confinements.

The dynamics of channels and bars over time were studied from the blueness images, which is a proxy for the channel depth. Blue represents the channel and white the bar. Changes in blueness values were used to study where erosion and sedimentation occurred in the experiment and to

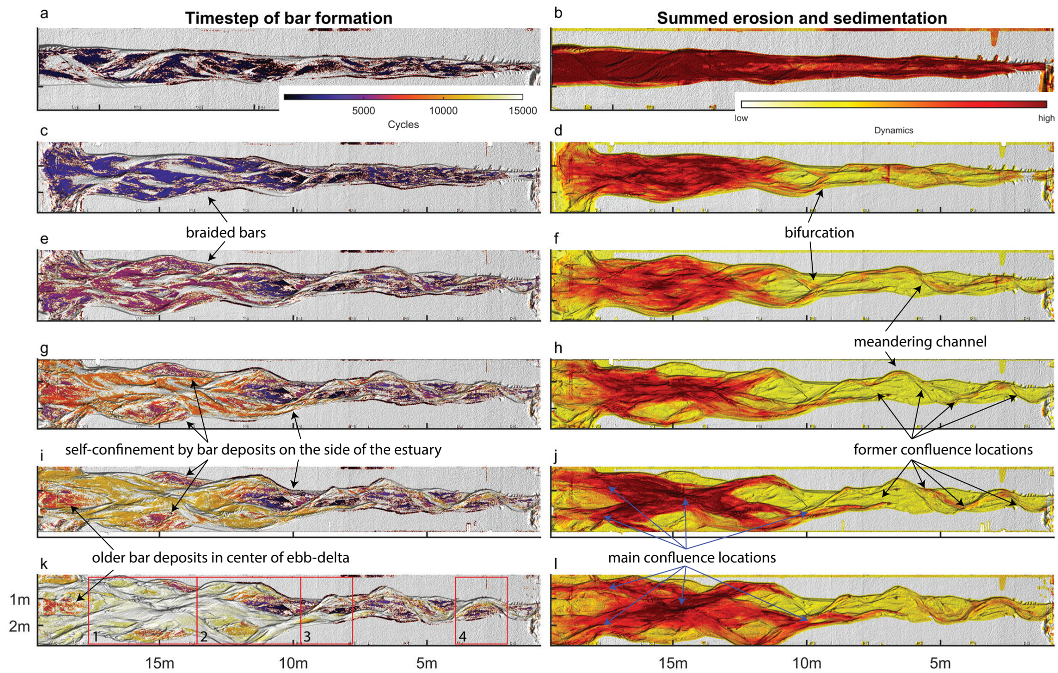

Figure 3. (left) Time step of last morphological activity, which indicate timing of bar formation and (right) morphodynamics represented by the sum of absolute bed level change. Maps for bar formation are given after 1250 (a), 3300 (c), 5900 (e), 8900 (g), 10900 (i) and 15000 (k). Summed erosion and deposition was calculated for the interval between two of these successive time steps and divided by the duration in tidal cycles. Red boxes in (k) show the zones for which hypsometric curves are calculated (Fig. 10c).

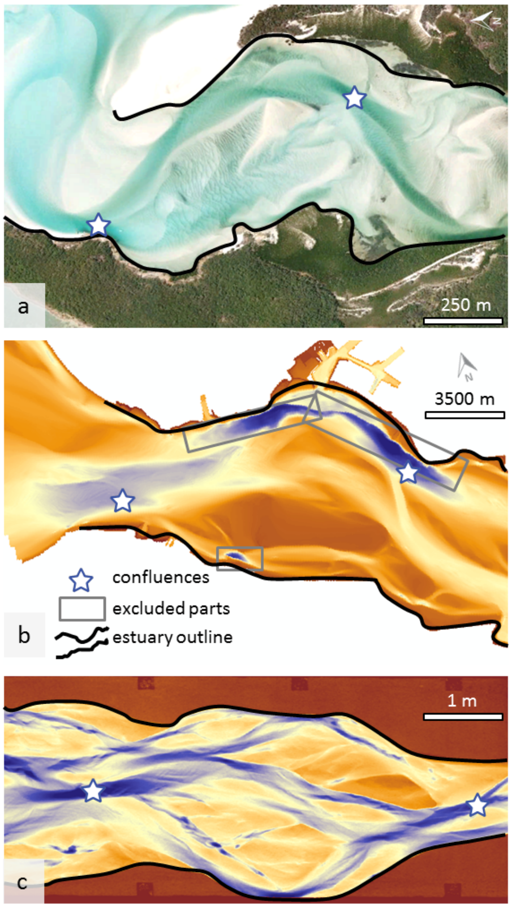

Figure 4. Locations of major confluences were determined in aerial photographs of natural systems (a), bathymetry of the Western Scheldt (b) and experiments (c). Warm colours denote high elevation, cool colours denote low elevation. In case of aerial photographs, major confluence locations were chosen as the deepest scour point where multiple channels converge. For the Western Scheldt and experiments, these locations were automatically extracted at the location of maximum depth from bathymetric data. For the Western Scheldt, deep scours as a result of bank protection or extensive shell deposits [*Cleveringa*, 2013] were excluded.

determine the time step of bar formation. The same approach was applied using successive DEMs of the experiment, but the temporal resolution for this was lower. Cumulative erosion and sedimentation was calculated as a measure of the spatial dynamics within the system and to assess whether the experiment was in dynamic equilibrium during the final stages. Cross-sectional profiles were taken from the LAB images and plotted over time, creating time-stack diagrams that show the migration of channels and bars in cross-section over time.

3 Results

3.1 General morphological evolution

In the initial phase of the experiment, an alternate bar pattern evolved (Figure 5a). As channel widening continued, a main meandering channel formed with riffles between two successive bends. The meandering channel forced the bars in specific locations, while lateral erosion and deposition increased the width of the forced bars. In a later stage, channels stabilised in the landward part of the estuary, while the channel width kept increasing in the seaward part. This allowed the development of multiple bars and channels in cross-section, which were first observed when flood barbs intersected the forced bars (Figure 5a,b). Barb channels are channels that become shallower in the direction of flow and have a dead end on the bar (Figure 5a). Net sediment transport towards the sea formed an ebb tidal delta that limited the inflow of water to the estuary. As widening progressed, forced mid-channel bars diverted the flow and periodically caused bank erosion. These zones were alternated by locations where the estuary width remained narrow or was self-confined by sidebar deposits, resulting in a quasi-periodic planform (Figure 5d,e).

3.2 Channel widening and incipient meandering

The initial phase of the experiment was characterised by the development of the initial converging channel into an incipient meandering ebb tidal channel (Figure 5a). In the first 200 cycles, the converging straight channel widened (Figure 6) and initially free alternate bars formed. The resulting channel pattern consisted of multiple straight channels parallel to the centreline of the estuary, which were separated by sills that connected the alternate bars in along-channel direction. Over time, the straight channels became more inclined and curved until they developed a meandering ebb tidal channel with shallow sills between adjacent channels, which forced the bars in place. On top of the alternate bars, circulating flow patterns developed, with residual currents dominantly going in landward direction onto the bars, then diverting to the channel and flowing back in seaward direction via the meandering channel (Figure 7a). Both the ebb and flood flows caused erosion of the estuary banks and migration of channels in the following tidal cycles (Figure 7b), while the forced bars increased in width until barb channels developed.

3.3 Alternate bars with initial barb formation

This phase was characterised by the formation of barb channels in the inner bends of the alternate bars. The main meandering ebb channel migrated laterally eroding the estuary banks and alternate bars grew in width. At the landward side shallow sills formed between two successive alternate bars. The sill separated the ebb flow from the flood flow in two separate channels. As the ebb channel migrated further seaward and the flood channel landward, u-shaped bars formed (Figure 5a). The u-shaped bars thereby partly blocked the channel with opposing flow (Figure 5a).

From 1000 tidal cycles onward the braiding index kept increasing as a result of the increasing channel width, which allowed for multiple braided bars (Figure 5a). Bars were particularly abundant in specific zones (at approximately 8 m, 11 m, 14 m and 15 m) where the summed width of bars was large (Figure 8a,b) and the compound bars were dissected by one or multiple barb channels. Between the zones with wide bar complexes, barb channels connected with

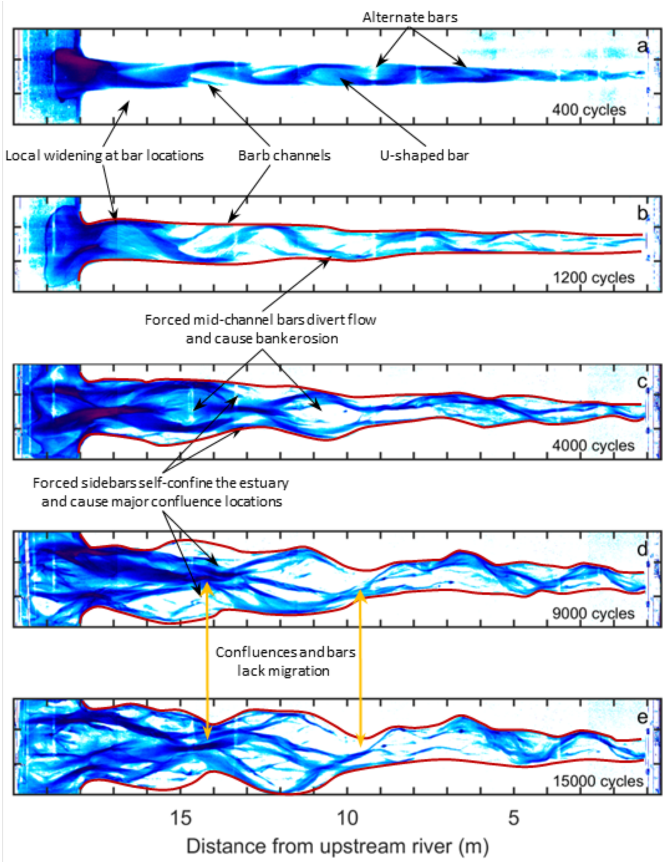

Figure 5. Time series of overhead imagery of the main experiment. Blueness is an indicator for channel depth. Estuary evolution started off with an initially straight converging channel, wherein an alternate bar pattern formed over the first 500 tidal cycles. See for all time-steps Supplementary Figure 2 or the Supplementary Movie.

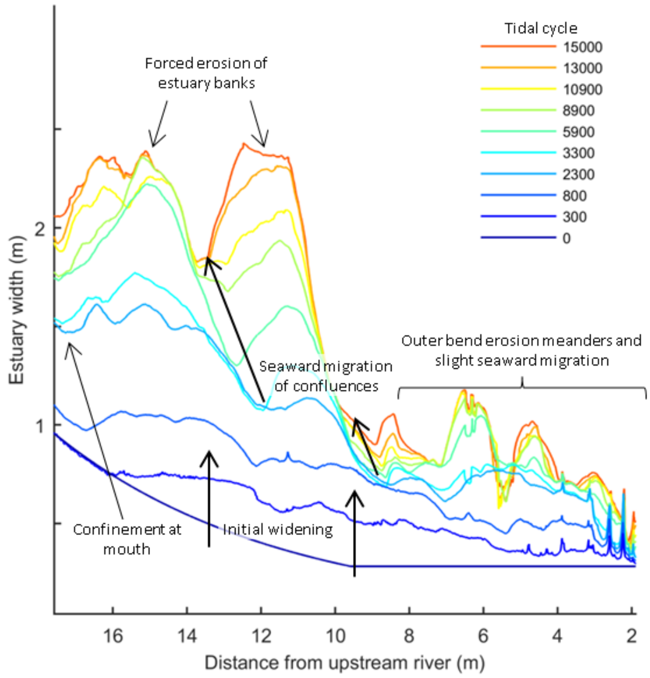

Figure 6. Evolution of the estuary width profile shows that after the initial widening an irregular planform evolved after 2300 cycles. After 3300 cycles, bars and landward meanders rapidly force local widening, while confinements migrate seaward. In the last phase, after 8900 cycles, the bars became static and bank erosion ceased at the confluence locations, while the amplitude of the quasi-periodic width variation increased at locations of bars.

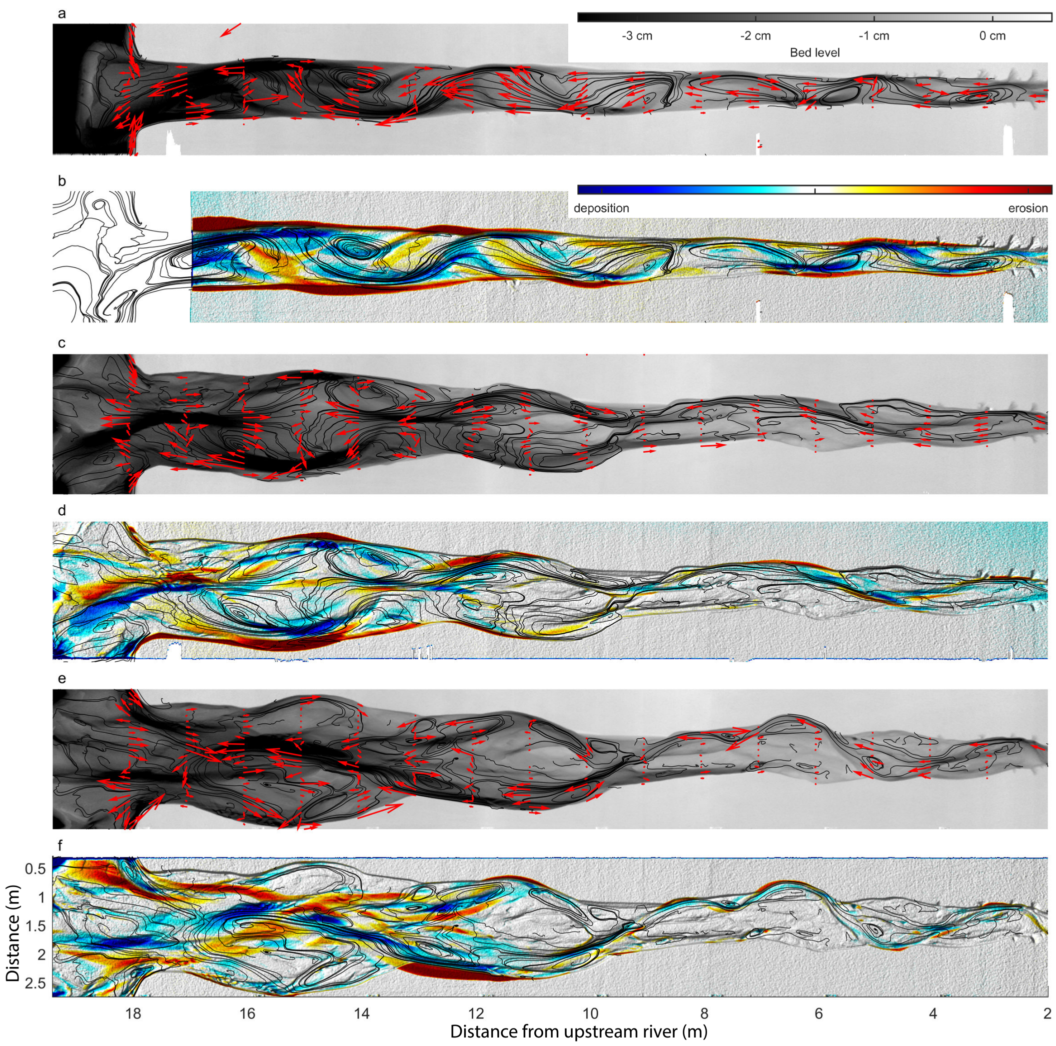

Figure 7. (a,c,e) Vectors indicating the residual currents after (a) 800, (c) 4400 and (e) 6900 cycles for transects with a spacing of a meter on top of a map with the streamlines based on a vector field with residual currents and the bathymetry. (b,d,f) Streamlines based on a vector field with residual currents, plotted on top of a map that indicates the erosion (red) and sedimentation (blue) in the subsequent phase of the experiment.

meandering ebb channels either during the ebb or flood phase, so that bars were generally less abundant.

At the seaward side, the export of sediment during the first 2000 cycles formed an ebb tidal delta. After this period, the delta was large enough to limit the inflow of water into the estuary, while erosion on the delta formed a single major channel at the northern side of the inlet (Supplementary Figure 2h,i). Connecting channels formed u-shaped bars that partly blocked the main channel and diverted the flow, which continuously resulted in outer-bend erosion and migration of the channels towards the sides of the estuary (2500-2700 cycles, Supplementary movie). This process initiated phases of noisy channel and bar patterns, alternating with more organised patterns with a main meandering channel and ebb and flood barbs that intersected the compound bars within the meander bends. Over time, channels evolved from a barb channel, ending on a sill or bar, to a main meandering channel and vice versa.

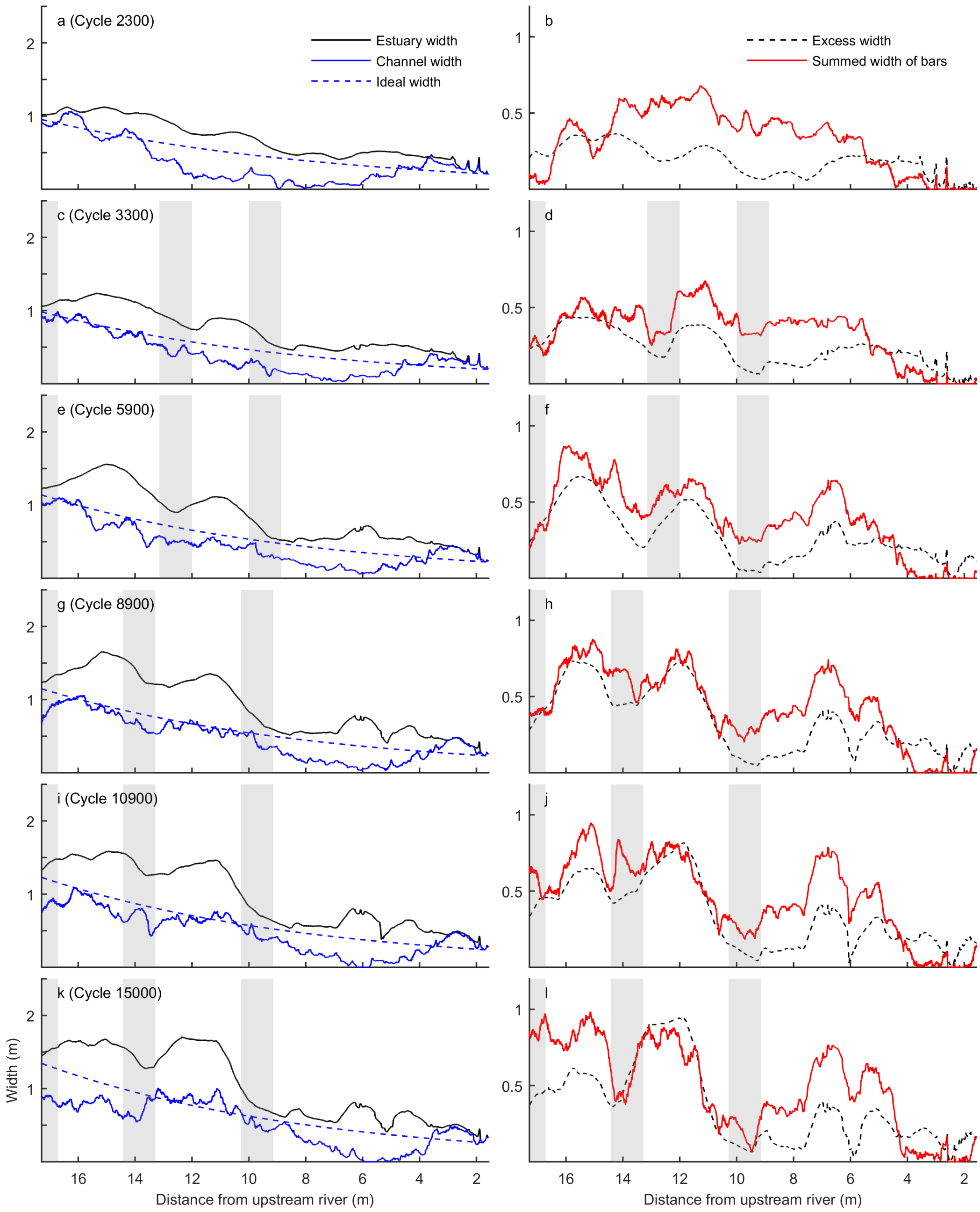

Figure 8. Evolution of estuary width, channel width and ideal width (left), and excess width and summed width of bars (right). Estuary width is the sum of channel and bar width. Ideal width is the largest fitting exponential shape in the estuary outline. Excess width is the estuary width minus the ideal width. The channel width approaches an ideal converging shape over time. Summed width of bars approaches the excess width. Shading indicates typical confinement locations where the summed channel width and summed bar width are relatively low.

The location of the main meandering channel shifted from north at 1000 cycles, to south around 2000 cycles and back north at about 3000 cycles at approximately 15 m from the upstream boundary (Supplementary Figure 2e,h,i). Interestingly, the adjacent channel confluence positions (at 13.5 m and at the mouth of the estuary) were relative stable over time, with dynamic bar and channel zones in between. This caused a rather irregular pattern in the outline of the estuary where some parts remained relatively narrow while other parts became relatively wide (Figure 6).

3.4 Mid-channel bars, confluences and evolution of quasi-periodic planform

In the central part of the estuary (8-18 m), widening resulted in the formation of forced mid-channel bars that triggered bank erosion and determined the location of confluences. For example after 4000 cycles, a large estuary width at 15 m allowed the existence of two major channels: one on the northern side and one on the southern side of the estuary, separated by a relatively wide bar in the centre of the estuary (Figure 5c). The confluences of these two channels occurred at the mouth of the estuary and at 13.5 m in a channel located in the middle of the estuary. While the two major channels at 15 m continued to migrate towards the outer banks of the estuary (Figure 9d), the bar between these channels obtained an oval shape as a result of an almost symmetrical ebb and flood barb on both its landward and seaward side. The residual current showed two major circulation cells at this bar complex (Figure 7c). The flood barb facilitated flow onto the bar, which diverged over the bar to the channels north and south of the bar. The ebb flow predominantly used the northern and southern channel around the bar and any flow entering the ebb barb also diverged into these channels. This caused bank erosion on both the north and south side of the estuary and sedimentation that increased the width of the mid-channel bar (Figure 7d). A similar process occurred in a more landward part slightly later in the experiment.

In the landward part of the estuary (0-8 m) the individual channels became more curved and connected, so that a main meandering channel formed from 5000 cycles onward (Figure 5c,d). The channel orientation of the upstream channel affected diversion of flow and sediment at the former bifurcation at 9 m, so that now the landward river system fed the southern branch instead of the northern branch (Figure 5c,d). This channel subsequently migrated (Figure 9c) by eroding the southern bank of the estuary at 10 m (Figure 7f), whereas the northern channel was only connected during flood flow. Seaward, the southern channel merged with the major channel that formed in the middle of the estuary at approximately 13 m. At this point multiple smaller barb channels formed onto the bar at 11 m that evaded each other and migrated over the bar.

At the mouth, the estuary was slightly narrower than the part of the estuary directly landward of the mouth at 16 m. Specific zones occurred where estuary width was relatively narrow with a major confluence and approached its ideal width. The zones were alternated by zones in which the estuary was much wider (Figure 8). Over time, the confluences migrated slightly seaward and the planform became progressively less ideal (Figure 6). The landward channel (0-8 m) eroded the estuary banks in the outer bends of the meanders until approximately 8000 tidal cycles. From that moment on the configuration of channels and bars in the landward part (0-8 m) remained relatively stable over time (Figure 5d,e,Figure 9a,b). In the seaward part of the estuary (12.5-18 m) and in the zone 9-13.5 m, the channels and bars were active over the full width. Two channels flowed around a fixated bar present in the middle of the estuary at 11 m (Figure 3b,d,f). The later phases of the experiment (6000-15000 cycles) were characterised by specific zones that were active (Figure 3h,j,l). These zones connected the major channel confluences at 10 m, 14 m and 18 m. The active zones were relatively narrow at locations where the confluences occurred (e.g. at 14 m and 18 m in Figure 3j) and relatively wide in the zones in between (e.g. at 16m).

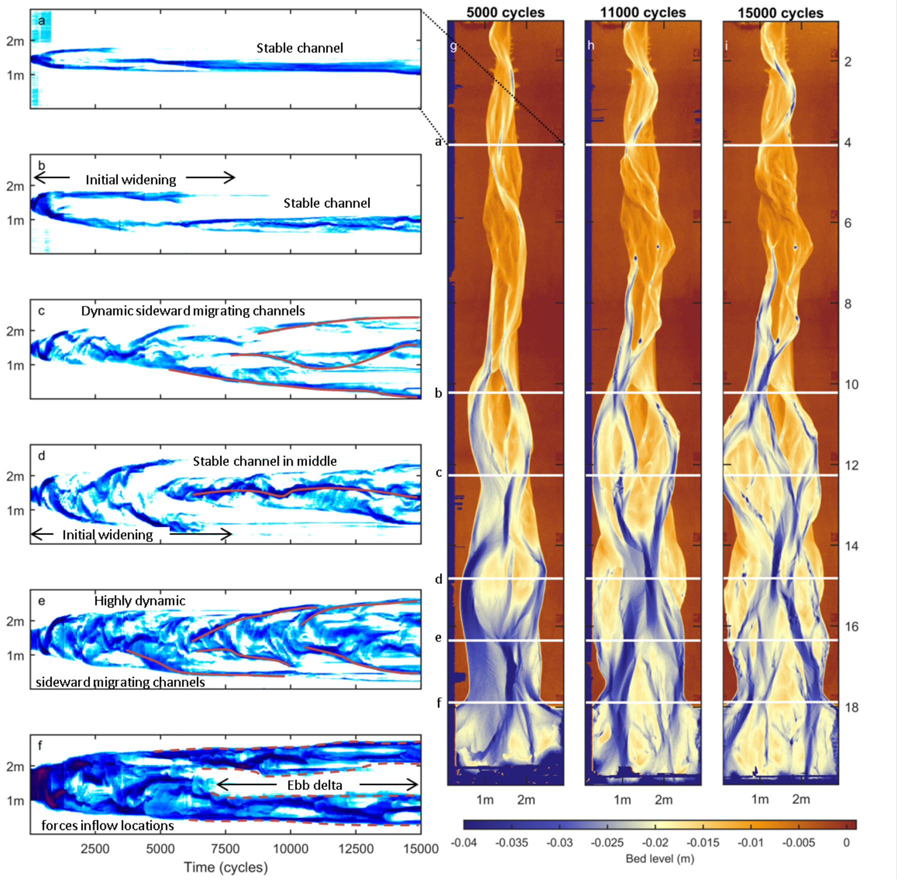

Figure 9. (a-f) Time-space diagrams of cross-sections in the experiment at 4 m, 10 m, 12 m, 14.5 m, 16 m and 17.5 m, which are indicated in (g,h,i) bathymetry after 5000, 11000 and 15000 tidal cycles. (a,b) A single landward channel stabilises from 7500 tidal cycles onwards. (c) In the centre, dynamic, sideward migrating channels occur. (d) Outward migrating channels erode the estuary banks. From about 6000 cycles the mid-channel bar is cross-cut and a single channel forms in the middle of the estuary. (e) In the seaward part, multiple very dynamic, migrating channels occur. The channels typically migrate from the centre towards the estuary banks. (f) An ebb delta formed and stabilised after 7500 tidal cycles. This forces the inflow on the sides of the ebb tidal delta.

3.5 Cross-cutting of mid-channel bars

In the seaward part, the phase with mid-channel bars and bank erosion continued until 5000 cycles, when a channel was able to progressively cut through the middle of the bar, connecting the barb channels around 5000-5500 cycles (Figure 5c,d). This caused a main channel along the centreline of the estuary. During this phase, the major in- and outflow was focused in the middle of the ebb tidal delta. This reduced bank erosion in the most downstream part of this estuary from that moment onward (Figure 6, 14-18 m), preventing the estuary shape from becoming more irregular.

In the central part of the estuary, the cross-cutting event also caused the direction of the residual circulation cells to reverse, with flood flows now predominantly occurring along the sides of the estuary, while the channel in the middle of the estuary was ebb dominant (Figure 7e). This reduced erosion of the estuary banks at this location and triggered the formation of new channels that connected the main ebb channel with the newly formed outflow locations on the ebb tidal delta (Figure 7f). Because the main channels in the middle of the seaward part of the estuary (14-18 m) gradually exported sediment to the central parts of the ebb tidal delta, this process eventually blocked the in- and outflow of water (6000-8000 cycles) (Supplementary Figure 2n-p). The ebb delta thus stabilised in place after 7500 tidal cycles (Figure9f,h), after which the in- and outflow of water became diverted to the northern and southern sides of the ebb tidal delta (Figure9f).

From about 7000 cycles onwards a single channel formed in the middle of the estuary, for which the position remained relatively stable over time (Figure 9d). Some minor secondary channels evolved on the sides in the final phase of the experiment, but their width was very small and their period of activity and migration very limited. In the part of the estuary between the confined and relatively stable zones (16 m), multiple very dynamic, migrating channels occurred. These channels typically originated in the centre of the cross-section after which they migrated laterally towards the estuary banks (Figure 9e).

Similarly to the previous bar cross-cutting event around 5000 cycles, a similar process occurred at the bar complex more landward (9.5-13 m), where after 9000 cycles the cross-cutting of the middle parts of the bar occurred (Figure 5d). This isolated a southern part of the bar complex at 9.5 m. In short, the estuary evolved from an initially converging channel into an estuary filled with bars that inherited its quasi-periodic planform from phases in which mid-channel bars diverted flow laterally, causing bank erosion.

3.6 Progressive infill from the sea and dynamic equilibrium with stable confluences

The channel width approached the ideal estuary width during the experiment (Figure 8) and the landward river and seaward delta stabilised in earlier phases (Figure 3). The zone between 4 and 8 m formed an exception, because bed levels in this zone were on average higher (Figure 9g,h,i) due to a set-up of water. In the final stage of the experiment (Figure 8k, Figure 6) the channel width in the seaward part of the estuary was smaller than the ideal width, because the ebb-tidal delta covered the full sea and sediment progressively filled the estuary in landward direction (Figure 5e).

The zones where the estuary was confined reflect the locations where bars were relatively less abundant. For natural systems it was found that tidal bars typically form at locations where the excess width is large, which is defined as the local estuary width minus the ideal estuary width [*Leuven et al.*, 2017]. This is in agreement with the experimental results (Figure 8f,h,j), where summed width of bars indeed approaches the excess width in the later stages of the experiment. While the zones between 4-8 m and 14-18 m deviated from this rule in magnitude, the direction of their along-channel profile is equal, i.e. low excess width corresponds to low summed width of bars and vice versa. Bed levels in these zones were on average higher due to a set-up of water, which possibly is caused by enhanced sedimentation in the middle of the flume for a lack of sediment input on the boundaries and an initial channel planform that deviates from the imposed flow conditions.

In the last phase, the estuary reached a dynamic equilibrium with stable confluences, while active channel migration remained in the parts between the confluences. Mean changes in bed level and sediment export illustrate that the experiment was close to dynamic equilibrium (Supplementary Figure 3). Generally, the increase in estuary width that was observed in previous stages decreased and only in the part 10-13 m and at the mouth of the estuary a slight increase in width occurred during the last 2000 cycles of the experiment (Figure 6).

In the final stages of the experiment, flow from the landward side bifurcated around the newly isolated bar at 11 m (10000-12000 cycles, Figure 5d,e), after which the northern branch began to erode the southern side of the former bar between 9.5 m and 12 m. At the same time the southern branch continued to erode the southern bank of the estuary until reaching the flume wall, which was the reason to end the experiment after 15000 cycles.

4 Discussion

This study presents the first experimental estuary with dynamic channels and bars, stable confluences, and a self-formed planform. The results show that the tides in combination with initial widening cause a pattern with forced mid-channel bars and confluences, which determine a quasi-periodic planform. Below, we first discuss the spatial and temporal scaling of bars. Second, the effect of bar patterns on the flow patterns is compared with the evolution of natural estuaries. Then, we describe a conceptual model on how forced bars determine the estuary outline. Last, the observed experimental cyclicity in channel and bar migration is compared to natural systems.

4.1 Spatial and temporal scales of channels and bars

The dimensions of tidal bars in the experiments scale well with bars observed in natural systems, as reported in *Leuven et al.* [2016] (Figure 10a). All experimental bars are within the uncertainty margins given for natural bars. However, most experimental bars plot above the trend line, indicating that their shape is slightly more elongated compared to the bars in natural systems (length-to-width ratio of approximately 8 in experiments, compared to 7 in nature). The difference is reasonable given the uncertainty margin of bar measurements in natural systems and the dependence of their dimensions on water level [*Leuven et al.*, 2016]. Moreover, the bar length is well within the range as expected based on local estuary width (Figure 10b). The experimental bars have similar dimensions as the alternate bar pattern reported in *Tambroni et al.* [2005] where the average bar wavelength is 3-6 times channel width, thus bar length is 1.5-3 times channel width. Most experimental bars fall exactly on the trend expected from natural systems. The largest outliers occur at the lower uncertainty band. These bars are an order of magnitude smaller than the other bars and formed in later phases of the experiment in one of the larger channel branches in the estuary. In this case, the width of the single branch is responsible for the bar dimensions. Therefore, scaling with the full estuary width may result in large deviations from the expected trend.

Hypsometric curves for four zones within the estuary (indicated in Figure 3k and Supplementary Figure 6a) show a large similarity between the experiment and the Western Scheldt (Figure 10e), where zones were defined as the estuary area between two successive confinements. Only zone 4 in the Western Scheldt deviates significantly from the hypsometry in the experiment (Figure 10e). At this location the estuary width is smaller and thus a larger part of the width is influenced by dredging to maintain shipping fairways. When channels are excluded and thus hypsometric curves are drawn for bar complexes only, bars in the Western Scheldt show a more linear elevation profile, while bars in the experiment have a more s-shaped curve (Figure 10f). The s-shaped curves for the experiment are caused by a small portion of the bar complexes being highly elevated and a small portion being very low elevated. High elevated

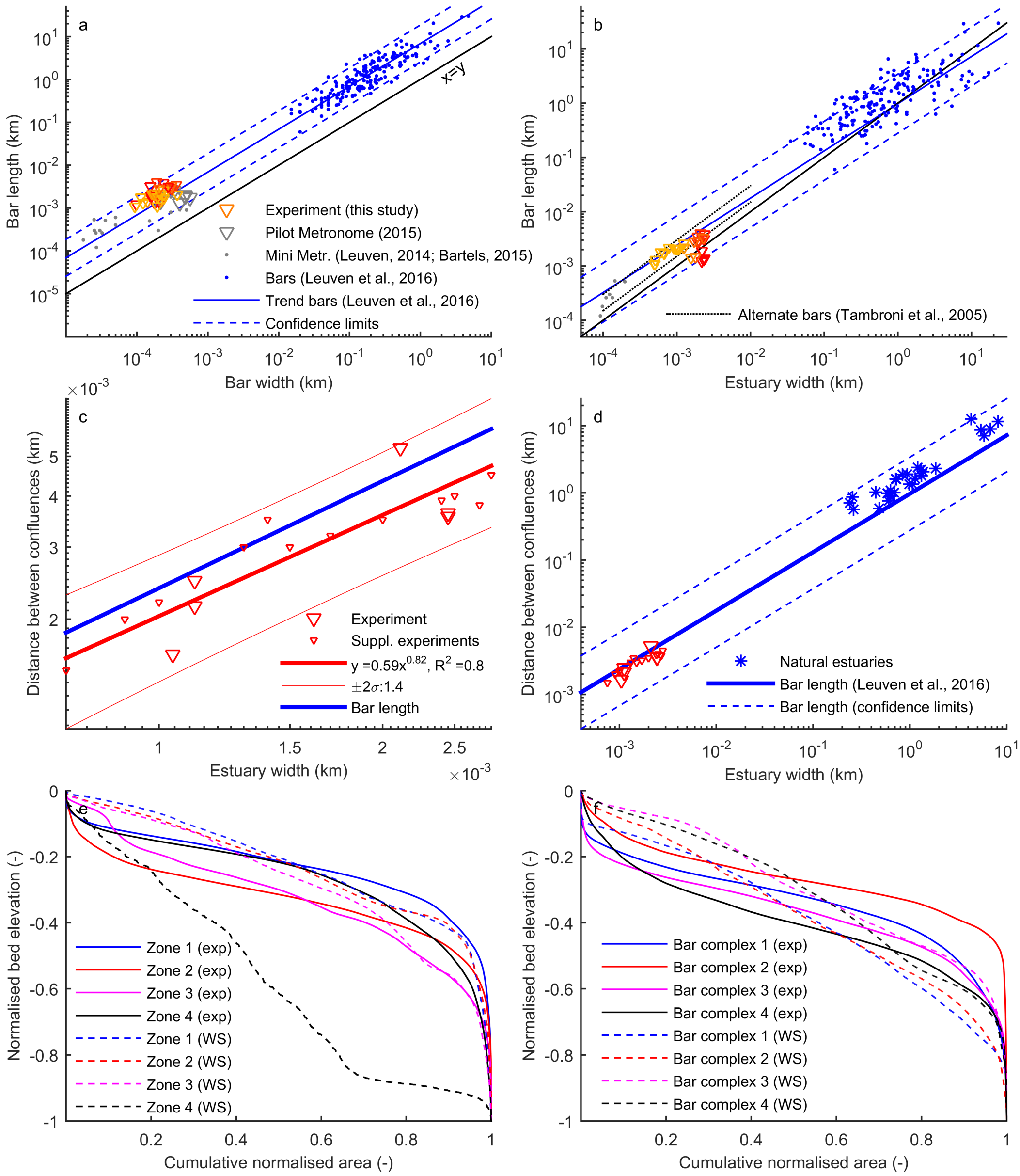

Figure 10. (a) Comparison of planform bar dimensions in experiments and natural systems. Triangles represent bars in the experiment. The redness of the triangles increases with the tidal cycle during which the bars were measured. (b) The scaling relation between estuary width and bar length that was found for natural systems holds for the experiments.(c) Confluence spacing as a function of local estuary width for experiments. Each triangle is the spacing between two successive confluences. (d) Comparison with natural systems. A line with predicted bar length ($\cdot 1.5$) is drawn for comparison and shows that confluence spacing scales with bar dimensions and estuary width. (e) Hypsometric curves of zones between two successive confinements in the estuary outline. The corresponding zones are given for the experiment in Figure 3k and for the Western Scheldt in Supplementary Figure 6a. Parts above the tidal range were excluded. (f) Hypsometric curves of bar complexes.

parts developed on the oldest parts of bars that accreted over time and lack flooding and morphodynamic activity in later phases. Low elevated parts are previous channels or scours on bars for which time was too short to fill in.

The experimental estuary shows a quasi-periodic shape that is narrow at confluences (Figure 6) and wide and dynamic between confluences (Figure 3). Because bars separate the major confluences, it is expected that confluence spacing scales with bar dimensions, which scale with estuary width (bar length $\propto$ channel width$^{0.87}$, *Leuven et al.* [2016]). This was found to be indeed the case (Figure 10c,d), which means that the spacing of confluences scales well with bar dimensions and estuary width. In general, this also implies a decreasing confluence spacing along-channel from the sea in landward direction, because channel and bar dimensions decrease. To quantify the location where confluences occur, we measured the distance from the location of the major confluences to the local minima in the outline of the estuary. The measured distance was normalised by the average spacing with the successive landward and seaward confluence locations. Results show that the major confluences in all cases occur within 16% of local confinements for the experiments and Western Scheldt over time, as well as for the aerial photographs of 8 natural systems (Supplementary Figure 4).

The timescale over which the channels and bars in the experiment evolve is 15000 tidal cycles, which corresponds to approximately 20 years of natural tidal cycles. The experimental estuary widens from a small initial channel by eroding its banks. All the eroded sediment is either exported to the ebb delta or used for bar formation. In contrast, most modern estuaries typically evolved over centuries to millennia during the middle to late Holocene under rising sea level [*van der Spek and Beets*, 1992; *Hijma and Cohen*, 2011; *de Haas et al.*, 2017]. As such, their evolution comprised many more tidal cycles than our experimental estuary. Most modern estuaries initially enlarged as former river valleys that drowned, because of the rapid sea-level rise around the start of the middle Holocene. Part of the slower evolution may thus be explained by the time required for aggrading after sea-level rise decreased, in contrast to the erosional behaviour in the experiment.

However, the experiment can be compared to the Western Scheldt, which evolved in the past 2700 years from a narrow creek in a peat bog to an alluvial estuary with a quasi-periodic planform (Figure 11). The timescale over which estuaries widen from a narrow creek after ingressions is typically in the order of hundreds of years, which may still be an estimate on the higher end for organic peat, which decays rapidly after erosion [*Pierik et al.*, 2017; *de Haas et al.*, 2017] and thus does not contribute to sediment available for bar formation. Despite their contrasting early evolution, the later stages of the experiment and natural systems were more similar. In that period the ebb and flood channels are dynamic, bars evolve and bank erosion causes a quasi-period planform. The relatively rapid evolution of bar patterns and bank erosion was also observed in river experiments and may partly be explained by a lack of bank strength in experiments without vegetation and cohesive material [*van Dijk et al.*, 2012].

Bar dynamics typically occurs in tidal inlets, embayments and estuaries on timescales from 15-40 years [*Israel and Dunsbergen*, 1999; *Levoy et al.*, 2017]. A comparison of the experiment with this timescale may be more appropriate, because these processes are not limited in sediment supply. Nevertheless, scaling relations for bar patterns in experiments [*Kleinhans et al.*, 2015a] and the natural processes that form bars [*Leuven et al.*, 2016] and confine estuaries are not well understood. Recent numerical models show that mud deposits may be required to confine estuary planform and that self-formed estuaries with mud can reach an equilibrium within 500-1000 years [*Braat et al.*, 2017].

4.2 Role of circulation cells and confluences on the evolution of estuaries

The historic evolution of channel and bar patterns in the Western Scheldt (1800-1900) was characterised by an initial phase of migration and meandering of the main ebb channels, after which the meander bends reached the embankments on the sides [*Jeuken*, 2000]. In the inner bends, the bar complexes extended laterally and flood barbs formed. This evolution is very similar to the initial phases of the experiment (Figures 6,11). However, after 1900, the morphological evolution was largely influenced by human interference: dikes were constructed, side branches that slowly filled-in were embanked and the first dredging activities started in 1922 [*Kleinjan*, 1938; *Jeuken*, 2000].

In 1944, *van Veen*, described the occurrence of circulation patterns in the Western Scheldt, where flow circulates through an ebb and a flood channel enclosing an intertidal bar. These circulation cells are similar to the circulation cells observed in the experiment, where the main meandering channel is ebb dominated and circulation cells covered the flood barb and adjacent ebb channel. These circulation cells divide the Western Scheldt into ca. 6 zones, which were later described as macrocells [*Winterwerp et al.*, 2001; *Toffolon and Crosato*, 2007; *Jeuken and Wang*, 2010; *Monge-Ganuzas et al.*, 2013]. These cells were determined using the morphology of the main ebb and flood tidal channels and residual flow, which resulted in cells that covered the enclosed area of an intertidal bar complex with its surrounding meandering channel. The boundaries of these cells in along-channel direction were chosen at the location of major channel confluences and correspond to the locations where the estuary width is relatively narrow. Typical recirculation patterns where observed within these cells [*Winterwerp et al.*, 2001], which may cause the observed dynamics of bars being relatively large compared to locations with major confluences (Supplementary Figure 6).

The concept of macrocells has so far only been applied to two natural systems – the Western Scheldt and the Oka estuary [*Winterwerp et al.*, 2001; *Toffolon and Crosato*, 2007; *Jeuken and Wang*, 2010; *Monge-Ganuzas et al.*, 2013], which are in a later stage of evolution because they have been filled with sediment over the Late Holocene [*van der Spek and Beets*, 1992; *Hijma and Cohen*, 2011]. However, the experimental results in this study show that already after 800 tidal cycles a set of serial circulation cells has evolved and that these circulation patterns can be used to explain how forced mid-channel bars cause bank erosion (Figure 7a,b).

After the experimental estuary became wide enough, a pattern with parallel circulation cells or cells with a mixed coupling [*Winterwerp et al.*, 2001] evolved (Figure 7c,e). Later phases of the experiment illustrated that the boundary of two successive circulation cells typically occurred at a major confluence and at locations where the estuary width is relatively narrow. These patterns resemble the patterns observed in the Western Scheldt (Supplementary Figure 6 and *van Veen* [1944]; *Winterwerp et al.* [2001]). Parallel and mixed coupling of circulation cells were found to be more resilient and are more likely to be preserved [*Winterwerp et al.*, 2001; *Wang and Winterwerp*, 2001]. This corresponds to our observations that over time, the positions of the confluences and local confinements stabilise in place and estuary bank erosion decreases (Figure 6).

A comparison of the Western Scheldt and the experiment shows that major confluences typically occur at locations where the width of the estuary is narrow (Figure 12a,b). Moreover, these are generally the locations where the active channel width, which is the estuary width over which erosion and sedimentation took place, and activity per pixel is relatively low (Figure 12c-f). Last, the number of channels and number of zones were sediment transport took place are relatively low for the locations of the major confluences (Figure 12i,j). This supports the hypothesis that the channels and bars are more dynamic in the zones between the confluences. While some noise is present, very similar trends are observed for the experiments (Supplementary Figure 5) and the Western Scheldt in activity (Figure 12) and evolution of width profiles (Figures 6,11).

4.3 Conceptual model for estuary planform forcing

We summarise the evolution of a self-formed estuary in a conceptual model containing three phases. In the first phase (Figure 13a) an alternate bar pattern develops, while the estuary widens. The initially straight channels connect to form a meandering channel, which results in outer bend erosion caused by bar push of the alternate bars [comparable to alternate bars in rivers *Struiksma et al.*, 1985; *Ikeda and Parker*, 1989; *Seminara and Tubino*, 1989; *van de*

Lageweg et al., 2014]. As soon as the bars exceed a width-to-length ratio of approximately 1/7, the flood flow is capable to form barb channels onto the alternate bars (Figure 13a). The barb channels progressively cut through the alternate bars. Both the outer bends of the meandering channels and the flood barbs erode the estuary banks, which creates an irregular estuary planform.

In phase II, the first mid-channel bars have formed that are large enough to divert the flow such that the outer bend erosion is accelerated and major confluences are formed seaward and landward of the mid-channel bars forming a quasi-periodic estuary planform (Figure 13b). At the confluence locations, estuary width generally remains narrow and dynamic channels and bars only occur within a small stretch of the estuary width. As outer bend erosion continues, the gradient over the mid-channel bar becomes favourable for both the ebb and the flood flows. These flows create new barb channels onto the mid-channel bar, which over time are capable to cross-cut the bar, forming a new main channel in the middle of the estuary (Phase III, Figure 13c). The timing of this event may vary along the estuary and confluences typically migrate seaward over the course of these phases.

After this phase, a dynamic equilibrium is reached, in which sediment from bars and banks is reworked into new bars within the estuary. The confluences remain stable and bank erosion is reduced. Dynamic zones of channels and bars typically occur in stretches between the major confluences. In both experiments and natural systems we observed the development of irregular estuary planforms and the forcing of channel confluences and zones with dynamic channels and bars. Observations in nature were based on historic maps of the Western Scheldt (Figure 11).

4.4 Cyclicity of channels and bars in tidal systems

Cyclicity is the periodic migration of channels and bars, in which the original configuration after a given period reoccurs. This has previously been reported for natural tidal systems as well as experiments. For example, experiments of short tidal basins show periodic migration of channels and shoals, which is coupled to reorganisation of the channels in the tidal basin [*Kleinhans et al.*, 2015b]. Most of the studies so far focussed on cyclicity on the ebb tidal delta [e.g. *Oost*, 1995; *Israel and Dunsbergen*, 1999; *Elias and van der Spek*, 2006], on which channels migrate from one side to the other, after which they disappear and reappear at their initial position. However, besides ebb deltas and the quasi-cyclic morphologic behaviour of the smaller-scale connecting channels that link the large ebb and flood channels in macro-cells [*van Veen*, 1950; *van den Berg et al.*, 1996; *Jeuken*, 2000; *Toffolon and Crosato*, 2007; *Swinkels et al.*, 2009; *de Vriend et al.*, 2011], little is known about the cyclicity of bars and channels within tidal basins or estuaries.

Levoy et al. [2017] observed an 18.6-year cycle in the migration of channels and tidal flats in the bay of Mont-Saint-Michel (France). They state that the periodic increase and decrease in flood-dominance corresponds with the periodic shift in the location of the channel, which is either located in the north or the south of the embayment. In this case, the bayward migration of tidal sand ridges forced a change in the in- and outflow direction of the tidal channels. It is hypothesised that a progressively northward swing of the northern channel configuration is caused by sand choking, i.e. a large sediment supply partly blocking the main channel. This latter mechanism could be similar to the observations in the final stage of the scale-experiments, in which the ebb tidal delta progressively expands in landward direction, followed by a southward migration of the channel at 11-12 m (Supplementary Figure 2s-u).

While not explicitly stated in the original paper [*Levoy et al.*, 2017], the presence of a monastery and some local bedrock in the middle of the entrance of the embayment may have had a forcing effect on the inflow location and direction of the tidal channels. Similarly, the local confinement present eastward in the embayment could force the main confluence location there. The observation in our experiments, where major confluences and narrow zones in the outline are self-formed thus fits with observations in this natural system. In addition, *Levoy et al.* [2017] recorded that infill of channels by reworking of bar sediments can cause sudden shifts of channels, which was also observed in the experiments when an ebb channel progressively blocks the evading flood channel by forming a u-shaped bar into that channel.

Our experimental results suggest that without any human interference (e.g. dredging or bank protection) the morphodynamics of macrocells remain active: the roles and locations of ebb and flood tidal channels may reverse within approximately 1000 tidal cycles and intertidal bars between these channels are continuously reworked. This is in contrast with natural systems under human interferences, in which dredging may cause degeneration of the affected cell and subsequently evolve into a single-channel system [*Wang and Winterwerp*, 2001; *Jeuken and Wang*, 2010; *Wang et al.*, 2015] and for which smaller connecting channels are disappearing by marsh formation on top of the shoals [*Swinkels et al.*, 2009]. Open questions include what the effect of dredging and dumping will be on the morphodynamics of estuaries and how an engineered estuary compares to a reference case with exactly the same initial and boundary conditions but without any human interference.

5 Conclusions

An experiment in a periodic tilting flume revealed the long-term evolution of channel and bar patterns in self-formed estuaries. Typically, in the landward part a main meandering channel forms that becomes stable over time, whereas in the seaward part dynamic channels and bars form that periodically shift laterally within the estuary. The intertidal bars are reworked and estuary banks are eroded in phases when forced mid-channel bars are present, which results in an estuary planform that is locally wider than the ideal converging shape. The seaward part can be subdivided in two zones with abundant and dynamic bars, which are separated by locations of channel confluences, at which the estuary is typically narrower. Lateral channel migration and bank erosion are caused by a gradual change in the inflow location and direction of the landward meandering channel and the in- and outflow locations on the ebb tidal delta. We conclude that stable confluence locations in self-formed estuaries are controlled by the spacing of tidal bars and that channels between the stable confluences are highly dynamic, which results in a quasi-periodic estuary planform.

The self-formed experimental estuary specifically shows that major confluences occur at relatively narrow parts in the estuary outline and that these confinements are self-formed by sidebar formation. This corresponds to observations in natural systems in which major confluences also occurred at self-formed confinements, for example by salt marsh formation, as well as forced confinements, for example by inherited geology or human engineering. However, natural channels and bars are limited in their dynamics, because channels are largely fixed or maintained in place. The spacing between two successive confluences is typically in the order of the estuary width, which indicates that confluence spacing scales well with bar and estuary dimensions. The experimental results and observations in natural systems suggest that an alternative quasi-periodic estuary planform evolves in self-formed alluvial estuaries in absence of any external forcing (geology, human influence), while the ideal estuary shape may be applicable to tidal creeks and branches of deltas in equilibrium.

Acknowledgments

This research was supported by the Dutch Technology Foundation TTW (grant Vici 016.140.316/13710 to MGK, which is part of the Netherlands Organisation for Scientific Research (NWO, and is partly funded by the Ministry of Economic Affairs). This work is part of the PhD research of JRFWL and LB. Reviewers will be acknowledged. We are grateful for technical support by Marcel van Maarseveen, Chris Roosendaal, Henk Markies and Arjan van Eijk. The authors contributed in the following proportions to conception and design, data collection and processing, analysis and conclusions, and manuscript preparation: JRFWL(55,45,75,75%), LB(5,45,0,0%), WMvD(5,5,10,10%), TdH(5,5,5,5%), MGK(30,0,10,10%). The data used are listed in the references, figures and supplements.

References

Agisoft, L., and R. St Petersburg (2017), Agisoft photoscan.

Ashmore, P. E. (2001), *Gravel-Bed River V*, chap. Braiding Phenomena: Statics and Kinetics, pp. 95–114, New Zealand Hydrological Society Inc., Wellington, New Zealand.

Baar, A., J. de Smit, W. Uijttewaal, and M. Kleinhans (2018), Sediment transport of fine sand to fine gravel on transverse bed slopes in rotating annular flume experiments, *Water Resources Research*, *54*, doi:https://doi.org/10.1002/2017WR020604.

Bartels, P. (2015), Ups-and-downs of tidal systems: formation and development of ebb-and flood tidal channels and bars., Master's thesis, Utrecht University.

Braat, L., T. van Kessel, J. R. F. W. Leuven, and M. G. Kleinhans (2017), Effects of mud supply on large-scale estuary morphology and development over centuries to millennia, *Earth Surface Dynamics Discussions*, *2017*, 1–47, doi:10.5194/esurf-2017-14.

Chandler, J. H., K. Shiono, P. Rameshwaren, and S. N. Lane (2001), Measuring flume surfaces for hydraulics research using a kodak dcs460, *The Photogrammetric Record*, *17*(97), 39–61.

Cleveringa, J. (2013), Ontwikkeling mesoschaal westerschelde - instandhouding vaarpassen schelde milieuvergunningen terugstorten baggerspecie (in dutch), *Tech. rep.*, ARCADIS.

de Haas, T., H. Pierik, A. van der Spek, K. Cohen, B. van Maanen, and M. Kleinhans (2017), Long-term evolution of tidal systems: effects of rivers, coastal boundary conditions, eco-engineering species, inherited relief and human interference, *Earth-Science Reviews*, *177*.

de Vriend, H. J., Z. B. Wang, T. Ysebaert, P. M. Herman, and P. Ding (2011), Eco-morphological problems in the yangtze estuary and the western scheldt, *Wetlands*, *31*(6), 1033–1042.

Elias, E. P., and A. J. van der Spek (2006), Long-term morphodynamic evolution of texel inlet and its ebb-tidal delta (the netherlands), *Marine Geology*, *225*(1), 5–21.

Fonstad, M. A., J. T. Dietrich, B. C. Courville, J. L. Jensen, and P. E. Carbonneau (2013), Topographic structure from motion: a new development in photogrammetric measurement, *Earth Surface Processes and Landforms*, *38*(4), 421–430.

Hijma, M. P., and K. M. Cohen (2011), Holocene transgression of the rhine river mouth area, the netherlands/southern north sea: palaeogeography and sequence stratigraphy, *Sedimentology*, *58*(6), 1453–1485.

Hundey, E., and P. Ashmore (2009), Length scale of braided river morphology, *Water Resources Research*, *45*(8).

Ikeda, S., and G. Parker (1989), *River Meandering*, American Geophysical Union.

Israel, C., and D. Dunsbergen (1999), Cyclic morphological development of the ameland inlet, the netherlands, in *Proceedings of Symposium on River, Coastal and Estuarine Morphodynamics (Genova, Italy)*, vol. 2, pp. 705–714.

Jeuken, M., and Z. Wang (2010), Impact of dredging and dumping on the stability of ebb–flood channel systems, *Coastal Engineering*, *57*(6), 553–566.

Jeuken, M.-C. J. L. (2000), *On the morphologic behaviour of tidal channels in the Westerschelde estuary*, Utrecht University.

Kleinhans, M., T. Van Rosmalen, C. Roosendaal, M. van der Vegt, et al. (2014a), Turning the tide: mutually evasive ebb-and flood-dominant channels and bars in an experimental estuary, *Advances in Geosciences*, *39*, 21–26.

Kleinhans, M. G., and J. H. van den Berg (2011), River channel and bar patterns explained and predicted by an empirical and a physics-based method, *Earth Surface Processes and Landforms*, *36*(6), 721–738, doi:10.1002/esp.2090.

Kleinhans, M. G., W. M. van Dijk, W. I. van de Lageweg, D. C. Hoyal, H. Markies, M. van Maarseveen, C. Roosendaal, W. van Weesep, D. van Breemen, R. Hoendervoogt, and N. Cheshier (2014b), Quantifiable effectiveness of experimental scaling of river-and delta morphodynamics and stratigraphy, *Earth-Science Reviews*, *133*, 43–61.

Kleinhans, M. G., C. Braudrick, W. M. Van Dijk, W. I. Van de Lageweg, R. Teske, and M. Van Oorschot (2015a), Swiftness of biomorphodynamics in lilliput-to giant-sized rivers and deltas, *Geomorphology*, *244*, 56–73.

Kleinhans, M. G., R. T. Scheltinga, M. Vegt, and H. Markies (2015b), Turning the tide: growth and dynamics of a tidal basin and inlet in experiments, *Journal of Geophysical Research: Earth Surface*, *120*(1), 95–119.

Kleinhans, M. G., M. van der Vegt, J. Leuven, L. Braat, H. Markies, A. Simmelink, C. Roosendaal, A. van Eijk, P. Vrijbergen, and M. van Maarseveen (2017a), Turning the tide: comparison of tidal flow by periodic sealevel fluctuation and by periodic bed tilting in the metronome tidal facility, *Earth Surface Dynamics Discussions*, *2017*, 1–35, doi:10.5194/esurf-2017-11.

Kleinhans, M. G., J. R. F. W. Leuven, L. Braat, and A. Baar (2017b), Scour holes and ripples occur below the hydraulic smooth to rough transition of movable beds, *Sedimentology*.

Kleinjan, I. (1938), Het gebied van de westerschelde nabij bath, *Rapport R88a, 88b, 88c. Rijkswaterstaat, Dordrecht*.

Lane, S., K. Richards, and J. Chandler (1993), Developments in photogrammetry; the geomorphological potential, *Progress in Physical Geography*, *17*(3), 306–328.

Langbein, W. (1963), The hydraulic geometry of a shallow estuary, *Hydrological Sciences Journal*, *8*(3), 84–94.

Leuven, J. (2014), Turning the tide: The effect of river discharge on estuary dynamics and equilibrium, Master's thesis, Utrecht University.

Leuven, J. R. F. W., M. G. Kleinhans, S. A. H. Weisscher, and M. van der Vegt (2016), Tidal sand bar dimensions and shapes in estuaries, *Earth-Science Reviews*, *161*, 204–233, doi:10.1016/j.earscirev.2016.08.004.

Leuven, J. R. F. W., T. Haas, L. Braat, and M. G. Kleinhans (2017), Topographic forcing of tidal sand bar patterns for irregular estuary planforms, *Earth Surface Processes and Landforms*.

Leuven, J. R. F. W., S. Selaković, and M. G. Kleinhans (2018), Morphology of bar-built estuaries: relation between planform shape and depth distribution, *Earth Surface Dynamics Discussions*, pp. 1–24, doi:10.5194/esurf-2018-18.

Levoy, F., E. Anthony, J. Dronkers, O. Monfort, G. Izabel, and C. Larsonneur (2017), Influence of the 18.6-year lunar nodal tidal cycle on tidal flats: Mont-saint-michel bay, france, *Marine Geology*, *387*, 108–113.

Mayor-Mora, R. E. (1977), Laboratory investigation of tidal inlets on sandy coasts., *Tech. rep.*, DTIC Document.

Monge-Ganuzas, M., A. Cearreta, and G. Evans (2013), Morphodynamic consequences of dredging and dumping activities along the lower oka estuary (urdaibai biosphere reserve, southeastern bay of biscay, spain), *Ocean & Coastal Management*, *77*, 40–49.

Morgan, J. A., D. J. Brogan, and P. A. Nelson (2017), Application of structure-from-motion photogrammetry in laboratory flumes, *Geomorphology*, *276*, 125–143.

Mori, N., and K.-A. Chang (2003), Experimental study of a horizontal jet in a wavy environment, *Journal of Engineering Mechanics*, *129*(10), 1149–1155.

Oost, A. P. (1995), Dynamics and sedimentary developments of the dutch wadden sea with a special emphasis on the frisian inlet: a study of the barrier islands, ebb-tidal deltas, inlets and drainage basins, Ph.D. thesis, Utrecht University.

Pierik, H., K. Cohen, P. Vos, A. van der Spek, and E. Stouthamer (2017), Late holocene coastal-plain evolution of the netherlands: the role of natural preconditions in human-induced sea ingressions, *Proceedings of the Geologists' Association*, *128*(2), 180–197.

Pillsbury, G. (1956), Tidal hydraulics. revised edition, corps of engineers, *US Army, May*.

Repetto, R., and M. Tubino (2001), Topographic expressions of bars in channels with variable width, *Physics and Chemistry of the Earth, Part B: Hydrology, Oceans and Atmosphere*, *26*(1), 71–76.

Reynolds, O. (1887), On certain laws relating to the regime of rivers and on the possibüity of experiments at small scale, *Brit. Ass. Report*.

Reynolds, O. (1889), On model estuaries in report of the committee appointed to investigate the action of waves and currents on the beds and fore shores of estuaries by means of working models, *Rept. Brit. Assoc*, pp. 327–343.

Savenije, H. H. (2015), Prediction in ungauged estuaries: An integrated theory, *Water Resources Research*, *51*(4), 2464–2476.

Schuurman, F., and M. G. Kleinhans (2015), Bar dynamics and bifurcation evolution in a modelled braided sand-bed river, *Earth Surface Processes and Landforms*, *40*(10), 1318–1333.

Schuurman, F., W. A. Marra, and M. G. Kleinhans (2013), Physics-based modeling of large braided sand-bed rivers: Bar pattern formation, dynamics, and sensitivity, *Journal of Geophysical Research: Earth Surface*, *118*(4), 2509–2527.

Schuurman, F., Y. Shimizu, T. Iwasaki, and M. Kleinhans (2016), Dynamic meandering in response to upstream perturbations and floodplain formation, *Geomorphology*, *253*, 94–109.

Seminara, G. (2010), Fluvial sedimentary patterns, *Annual Review of Fluid Mechanics*, *42*, 43–66.

Seminara, G., and M. Tubino (1989), *River meandering*, chap. Alternate bars and meandering: free forced and mixed interactions, pp. 267–320, American Geophysical Union.

Stefanon, L., L. Carniello, A. DŠAlpaos, and S. Lanzoni (2010), Experimental analysis of tidal network growth and development, *Continental Shelf Research*, *30*(8), 950–962.

Struiksma, N., K. Olesen, C. Flokstra, and H. De Vriend (1985), Bed deformation in curved alluvial channels, *Journal of Hydraulic Research*, *23*(1), 57–79.

Swinkels, C. M., C. M. Jeuken, Z. B. Wang, and R. J. Nicholls (2009), Presence of connecting channels in the western scheldt estuary, *Journal of Coastal Research*, pp. 627–640.

Tambroni, N., M. Bolla Pittaluga, and G. Seminara (2005), Laboratory observations of the morphodynamic evolution of tidal channels and tidal inlets, *Journal of Geophysical Research: Earth Surface*, *110*(F4).

Toffolon, M., and A. Crosato (2007), Developing macroscale indicators for estuarine morphology: The case of the scheldt estuary, *Journal of Coastal Research*, *23*(1), 195–212.

Townend, I. (2012), The estimation of estuary dimensions using a simplified form model and the exogenous controls, *Earth Surface Processes and Landforms*, *37*(15), 1573–1583.

Tubino, M., R. Repetto, and G. Zolezzi (1999), Free bars in rivers, *Journal of Hydraulic Research*, *37*(6), 759–775.

van de Lageweg, W. I., W. M. van Dijk, A. W. Baar, J. Rutten, and M. G. Kleinhans (2014), Bank pull or bar push: What drives scroll-bar formation in meandering rivers?, *Geology*, *42*(4), 319–322.

van den Berg, J. H., C. J. Jeuken, and A. J. Van der Spek (1996), Hydraulic processes affecting the morphology and evolution of the westerschelde estuary, in *Estuarine Shores: Evolution, Environments and Human Alterations*, edited by K. F. Nordstrom and C. T. Roman, pp. 157–184, John Wiley & Sons Ltd.

van der Spek, A. J., and D. J. Beets (1992), Mid-holocene evolution of a tidal basin in the western netherlands: a model for future changes in the northern netherlands under conditions of accelerated sea-level rise?, *Sedimentary Geology*, *80*(3), 185–197.

van der Wegen, M., and J. Roelvink (2012), Reproduction of estuarine bathymetry by means of a process-based model: Western scheldt case study, the netherlands, *Geomorphology*, *179*, 152–167.

van Dijk, W. M., W. I. van de Lageweg, and M. G. Kleinhans (2012), Experimental meandering river with chute cutoffs, *Journal of Geophysical Research: Earth Surface*, *117*(F3), n/a–n/a, doi:10.1029/2011JF002314, f03023.

van Dijk, W. M., W. I. Lageweg, and M. G. Kleinhans (2013), Formation of a cohesive floodplain in a dynamic experimental meandering river, *Earth Surface Processes and Landforms*, *38*(13), 1550–1565.

van Veen, J. (1944), Schelderegiem en schelderegie, *Tech. rep.*, Rijkswaterstaat reprint 1993, Middelburg.

van Veen, J. (1950), Eb-en vloedschaarsystemen in de nederlandse getijwateren, *Tijdschrift Koninklijk Nederlands Aardrijkskundig Genootschap*, *67*, 303–325.

Vlaswinkel, B. M., and A. Cantelli (2011), Geometric characteristics and evolution of a tidal channel network in experimental setting, *Earth Surface Processes and Landforms*, *36*(6), 739–752.

Wang, Z., and J. Winterwerp (2001), Impact of dredging and dumping on the stability of ebb-flood channel systems, in *Proceedings of the 2nd IAHR symposium on River, Coastal and Estuarine Morphodynamics*, pp. 515–524.

Wang, Z., D. Van Maren, P. Ding, S. Yang, B. Van Prooijen, P. De Vet, J. Winterwerp, H. De Vriend, M. Stive, and Q. He (2015), Human impacts on morphodynamic thresholds in estuarine systems, *Continental Shelf Research*, *111*, 174–183.

Westoby, M., J. Brasington, N. Glasser, M. Hambrey, and J. Reynolds (2012), Śstructure-from-motionŠphotogrammetry: A low-cost, effective tool for geoscience applications, *Geomorphology*, *179*, 300–314.

Winterwerp, J., Z. Wang, M. Stive, A. Arends, C. Jeuken, C. Kuijper, and P. Thoolen (2001), A new morphological schematization of the western scheldt estuary, the netherlands, in *Proceedings of the 2nd IAHR symposium on River, Coastal and Estuarine Morphodynamics*, pp. 525–533.

Wu, F.-C., Y.-C. Shao, and Y.-C. Chen (2011), Quantifying the forcing effect of channel width variations on free bars: Morphodynamic modeling based on characteristic dissipative galerkin scheme, *Journal of Geophysical Research: Earth Surface*, *116*(F3).

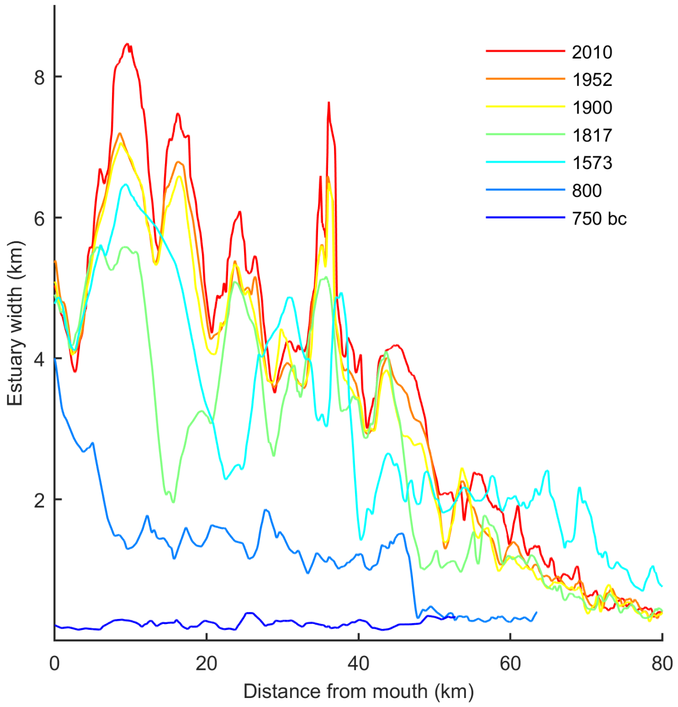

Figure 11. Evolution of the estuary width profile of the Western Scheldt (The Netherlands) shows a similar evolution as the experiment.

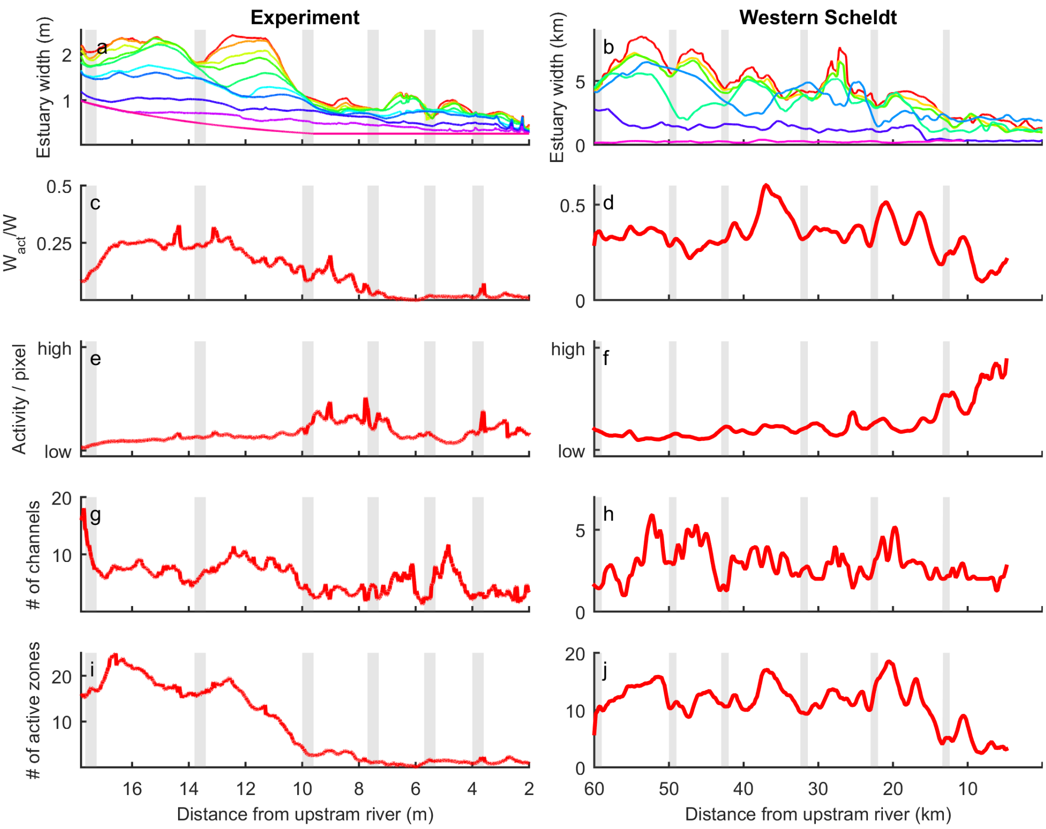

Figure 12. Along channel variation for the experiment (left) and Western Scheldt (right). (a,b) local estuary width over time. (c,d) Time-averaged active channel width normalised with local estuary width. (e,f) Sum of absolute bed level change per pixel. (g,h) Number of channels in cross-section. (i,j) Number of active areas in cross-section. Shading indicates typical confinement locations where the active width, activity per pixel and number of channels are generally low. The along-channel profiles (c-j) were averaged over the period 7500-15000 cycles for the experiment and the years 2000-2015 for the western Scheldt.

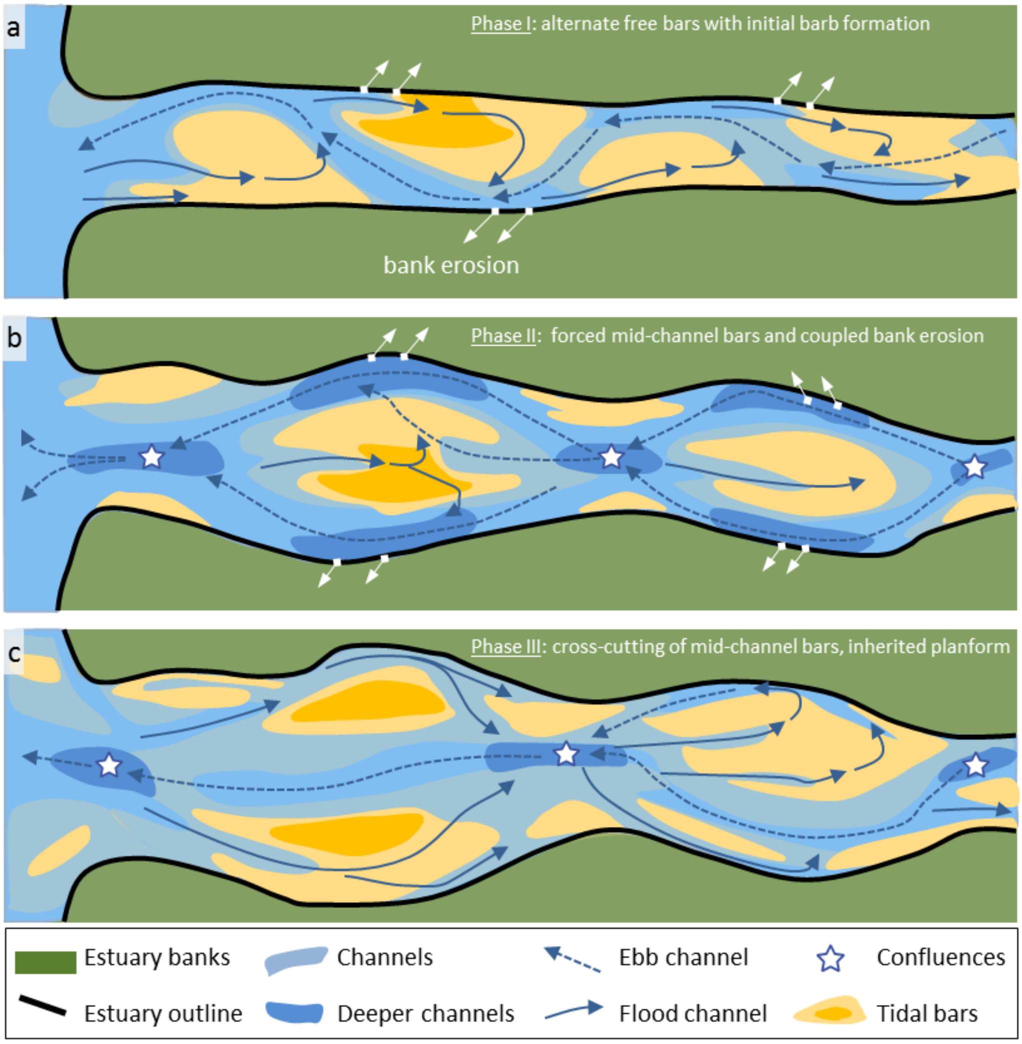

Figure 13. Conceptual model for estuary planform development influenced by forced bars. (a) Phase I: the initial converging channel widens and free alternate bars form. The meandering channel around the alternate bars is predominantly used as ebb channel, eroding the outer bends. While the alternate bars widen, initial flood barbs form onto the alternate bars. (b) Phase II: The flood barb channels progressively cut through the alternate bars, isolating forced mid-channel bars in the middle of the estuary. This creates two major confluences, one at the mouth and one upstream of the mid channel bar. The flow is forced around the mid-channel bar, which causes bank erosion, resulting in an even more irregular planform. (c) Phase III: Barb channels on the mid-channel bar enlarge and subsequently connect, cross-cutting the bar. This forms a new channel in the middle of the estuary and limits the erosion of the estuary banks. The resulting quasi-periodic planform is inherited from phase II. Major confluences separate zones in which channels periodically rework tidal bars.